Pharm Res (2014) 31:322–334
DOI 10.1007/s11095-013-1162-9

RESEARCH PAPER

Fucosylated Multiwalled Carbon Nanotubes for Kupffer Cells Targeting for the Treatment of Cytokine-Induced Liver Damage

Richa Gupta • Neelesh Kumar Mehra • Narendra Kumar Jain

Received: 19 April 2013 / Accepted: 28 July 2013 / Published online: 17 September 2013

ABSTRACT

Purpose To develop, characterize and exploring the sulfasalazine loaded fucoyslated multi walled carbon nanotubes for Kupffer cell targeting for effective management of cytokine-induce liver damage.

Methods Sulfasalazine was loaded into the fucosylated MWCNTs after subsequential functionalization (carboxylation, acylation and amidation) using dialysis membrane technique. The *in vitro*, *in vivo* studies were performed on macrophages J 774 cell line for Kupffer cells targeting for the treatment of cytokine-induced liver damage.

Results The loading of SSZ into SSZ-FUCO-MWCNTs was 87.77 ± 0.11% ($n = 3$). Sustained release was obtained from SSZ-FUCO-MWCNTs, with 89.12 ± 0.71% of SSZ released into medium at 48th hr. SSZ-FUCO-MWCNTs showed the 9.01 ± 0.23% hemolysis was drastically reduced from 21.62 ± 0.24% SSZMWCNTs 21.62 ± 0.24%. In SRB assay, SSZ-FUCO-MWCNTs showed more cytotoxicity than raw and SSZ-MWCNTs. In cytokine assay, SSZ- FUCO-MWCNTs exhibited significantly higher inhibition of IL-12 p40 secretion. In Western blot assay, SSZ-FUCO-MWCNTs significantly inhibit NF-κB activation.

Conclusion The results suggested that the SSZ-FUCO-MWCNTs may be useful nano-carriers for targeted delivery to Kupffer cells in the treatment of cytokine-induced liver damage.

KEY WORDS carbon nanotubes · fucose · Kupffer cells · liver targeting · sulfasalazine

R. Gupta · N. K. Mehra (✉) · N. K. Jain (✉)
Pharmaceutics Research Laboratory
Department of Pharmaceutical Sciences, Dr. H. S. Gour University
Sagar, MP 470 003, India
e-mail: neelesh81mph@gmail.com
e-mail: jnarendr@yahoo.co.in

INTRODUCTION

Nuclear factor-κB (NF-κB) resides in the cytoplasm of virtually all cell types in an inactive form, where it is associated with regulatory protein, called inhibitory proteins (IkBα and IkBβ), and this association prevents the entry of NF-κB into the nuclei. The term NF-κB is a collective name for inducible dimeric transcription factor that consists of five Rel subunits, namely p50, p52, RelA (also known as p65), RelB and c-Rel, expressed in the cytoplasm of Kupffer cells (macrophages of liver). It plays crucial role in inflammatory liver signaling because NF-κB is one of the most important regulators of pro-inflammatory gene expression. Kupffer cells get stimulated upon exposure of pathogens like bacteria and viruses, and as a result, transcription factor, nuclear factor κB (NF-κB) is activated. Upon stimulation, Kupffer cells release the specific kinase that phosphorylates IκB and causes its rapid degradation by proteasomes (1–3). The release of NF-κB from IκB results in the passage of NF-κB into the nucleus, where it binds to specific sequences in the promoter regions of target genes. As a consequence, inflammatory proteins such as chemokines and cytokines like interleukins (IL-6 and IL-12) and tumor necrosis factor α (TNF-α) are released (4,5) (Scheme 1). Since activated NF-κB mediates the production of inflammatory cytokines, it brings the need for selective targeting of NF-κB in Kupffer cells for treatment of cytokine-induced liver damage (6). Hence the delivery of an NF-κB inhibitor drug to Kupffer cells seems to be an attractive option for the treatment of the disease.

We have chosen a sulfasalazine (SSZ) anti-inflammatory, a potent NF-κB inhibitor (7). It inhibits NF-κB dependent transcription in micro- to milli- molar concentrations, conversely 5-ASA or sulfapyridine SP does not block NF-κB activation at all doses (8). SSZ inhibits phosphorylation of IκB thus the nuclear localization of NF-κB is subdued and as a result no cytokine production takes place (9). However SSZ depicted the dose dependent side effects (10). Hence decrease in dose of drug and prevention or minimizing its action on non-target

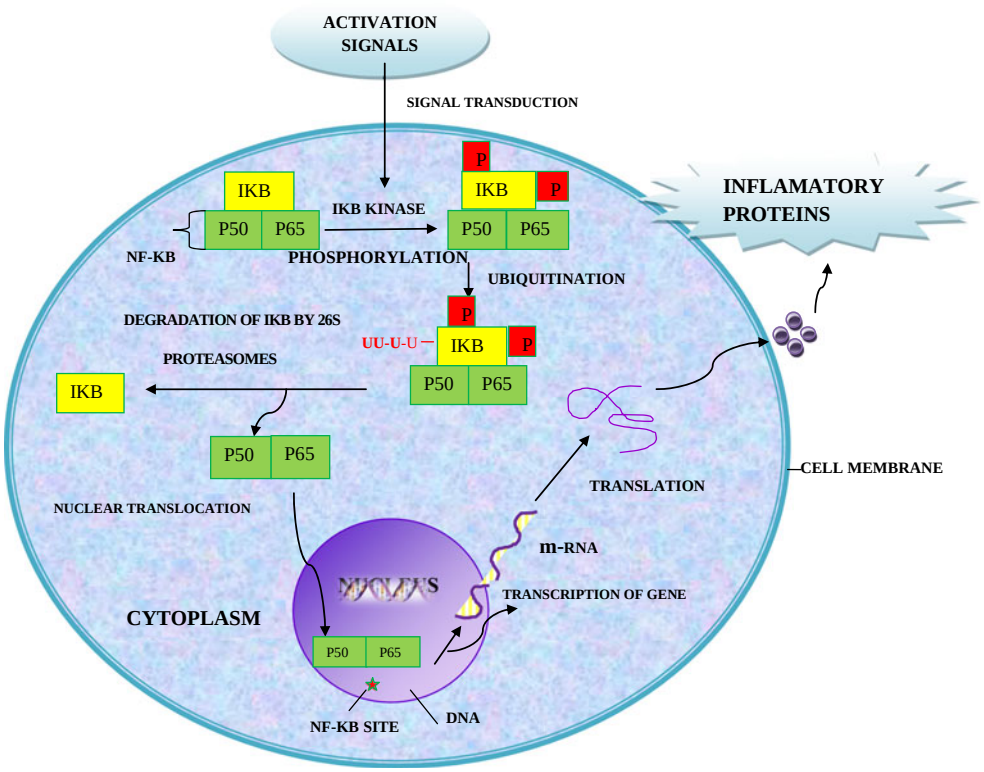

Scheme I Schematic diagram of NF-KB activation.

cells should also reduce the harmful side effects. Kupffer cells possess various receptors on their outer membrane that recognize carbohydrate derivatives. The surface modified carriers with mannose and fucose residues are taken up by macrophages at higher rates (11). Therefore, targeting of NF-κB inhibitor drug to activated macrophages could be an attractive approach in improving the therapeutic efficacy and reducing the toxicity of NF-κB inhibitor bioactive.

In the current scenario, carbon nanotubes have emerged as most advanced nano-carrier in targeted drug delivery, attributed to their nano-size and tiny needle tubular structure, high surface area to volume ratio and ability to entrap higher amount of bioactives in them (12–18). Depending upon their atomic layer arrangements carbon nanotubes are: single-, double- and multi-walled; SWCNTs, DWCNTs, and MWCNTs, respectively. Particularly, MWCNTs have become the most attractive carbon nanostructure in targeted delivery due to its extremely large surface areas, low cost, good biocompatibility, excellent loading efficiency and deliver drug into the specific cells.

The synthesized, first generation or pristine carbon nanotubes are hydrophobic in nature and not suitable for drug delivery, thus surface modifications render them hydrophilic and make them suitable for targeted delivery. For targeted delivery the targeting ligand including dexamethasone, carbohydrates, vitamins *etc.* are attached on to the terminal portion of the surface engineered nanotubes (19–24). Higuchi *et al.* investigated potential role of fucose anchored cationic liposome/NF-κB decoy complexes in the treatment of cytokine-related liver disease (25). Fucose had been shown to be a most promising ligand among various ligands investigated so far, for macrophage targeting because the macrophages possess a large number of receptors that can be easily recognized by carbohydrate units. Therefore, we hypothesized that MWCNTs can be a better alternative and promising carrier for targeting the macrophages of liver. Thus the purpose of the present investigation is to explore the targeting potential and NF-κB inhibition activity of sulfasalzine loaded fucosylated multi-walled carbon nanotubes (SSZ-FUCO-MWCNTs) as compared to free SSZ and unconjugated MWCNTs. To best of our knowledge this is the debut report that explores carbon nanotubes for Kupffer cells targeting. The various MWCNTs formulations were prepared and characterized for entrapment efficiency, *in-vitro* release, stability and hemolytic toxicity. *Ex-vivo* cytotoxicity, cellular uptake and NF-κB inhibition were studied against macrophage cell line J774. Finally, *in-vivo* pharmacokinetic, biodistribution and hematological parameters were also evaluated for free SSZ and MWCNTs formulations.

MATERIALS AND METHODS

Materials

L-fucose and Dialysis membrane (MWCO, 12–14 KDa) were purchased from HiMedia Laboratories Pvt. Ltd. Mumbai, India. Ethylenediamine (EDA) and acrylonitrile were

purchased from Central Drug House (CDH), New Delhi, India. Polytetra fluoro ethylenes (PTFE) filters of 0.45 µm pore size was purchased from Rankem (India). Multi Walled Carbon Nanotubes (MWCNTs) produced by chemical vapor deposition (CVD) with purity 99.3% and diameter × length 110–170 nm × 5–9 µm were purchased from Sigma Aldrich Pvt. Ltd. (USA). All other chemicals were of analytical grade and purchased from CDH, (India).

Purification and Functionalization of MWCNTs

Purification of MWCNTs was performed using previously reported method with slight modification (23,24,26). As-received 500 mg of MWCNTS was kept in hot air oven (Hot Air Sterilizer, Yorco, India) at 250±2°C for 1 h, filtered through PTFE filter (0.45 µm, Rankem, India), dried in a vacuum oven (Jyoti Scientific Industries, Gwalior, India) and collected.

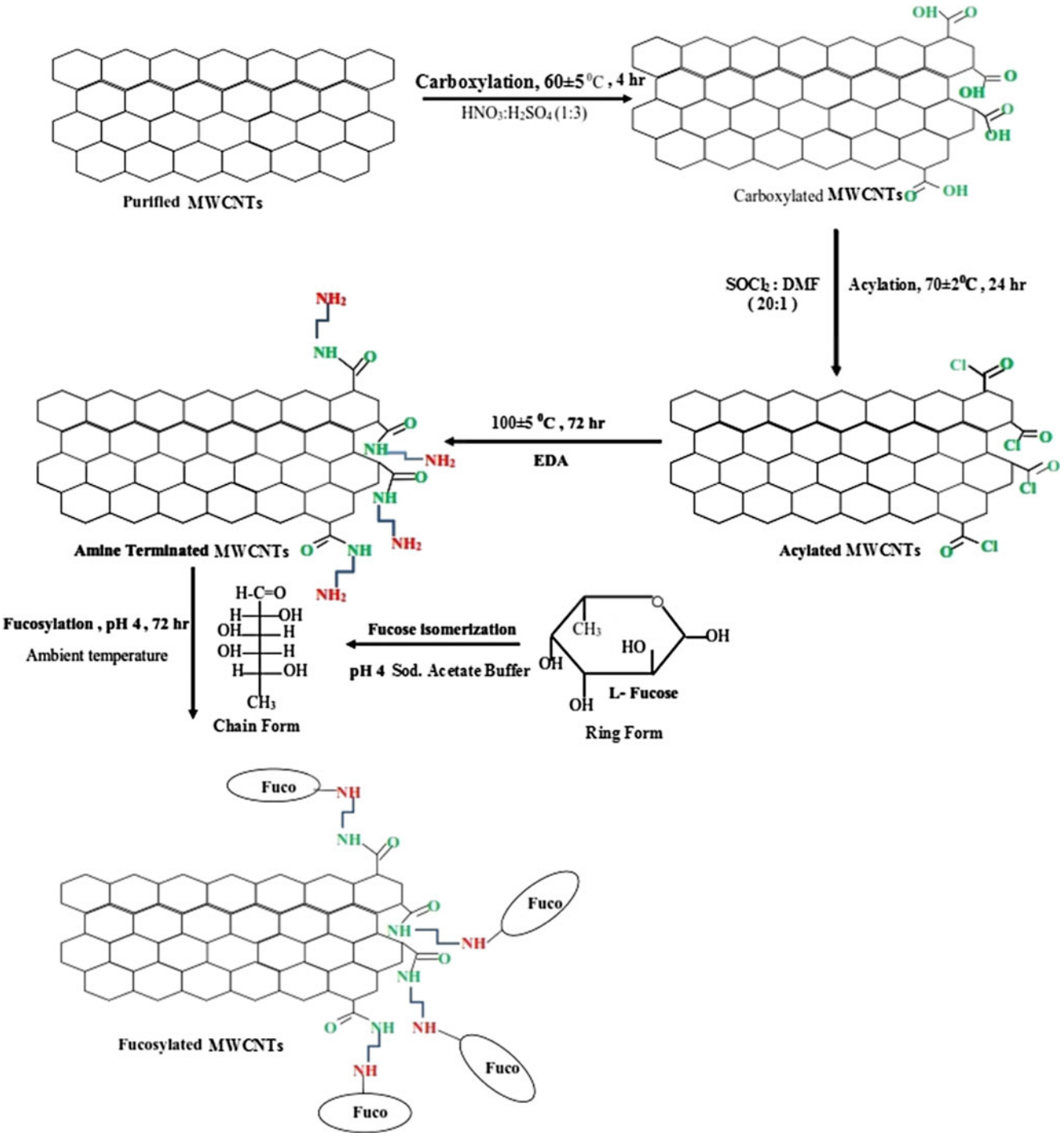

Scheme 2 Functionalization and fucosylation of MWCNTs (19,23).

Carboxylation of the purified MWCNTs was done according to the previously reported method (19,22–24,27) with slight modifications. For this, 300 mg of purified MWCNTs was refluxed in a mixture of concentrated nitric acid and sulphuric acid (HNO_3:H_2SO_4::1:3) at 60±5°C for 4 h. After refluxing, MWCNTs was washed with deionized water several times until neutral pH was attained. Carboxylated MWCNTs was filtered using PTFE filter (0.45 μm, Rankem, India), washed and finally dried in a vacuum oven (Jyoti Scientific Industries, Gwalior, India).

The carboxylated MWCNTs was acylated and amidated according to the previously reported methods from our laboratory (19,23,24). Carboxylated MWCNTs (100 mg) was stirred magnetically in a mixture of thionyl chloride ($SOCl_2$) and N, N-dimethyl formamide (DMF) in 20:1 volume ratio at 70±2°C for 24 h. After acylation MWCNTs was filtered, washed with anhydrous tetrahydrofuran (THF) several times, and dried. Acylated MWCNTs (50 mg) was reacted with excess ethylene diamine (EDA) solution using DMF as a solvent at 100±5°C for 72 h. The excess amount of ethylene diamine was washed with DMF followed by anhydrous THF, filtered and dried in a vacuum oven (Jyoti Scientific Industries, Gwalior, India).

Fucosylation of Functionalized MWCNTs

Fucosylation of the amine terminated MWCNTs was carried out in sequential steps as shown in Scheme 2 in accordance with the previously reported method (19,23,28), with slight modification. Briefly, L-fucose (8 μM) was dissolved in sodium acetate buffer (pH 4.0; 0.1 M), added to lyophilized amine modified MWCNTs, followed by heating at 60±0.5°C for an hr. The mixture was agitated on a magnetic stirrer at room temperature (25±2°C) for 72 h to ensure the completion of reaction. Fucosylated MWCNTs (FUCO-MWCNTs) was purified by dialyzing in a dialysis tubing (MWCO 12–14 KDa) against deionized water for 24 h to eliminate the unconjugated fucose along with other impurities, which diffuse out into water and finally, FUCO-MWCNTs was retained inside. The dialyzed nanoconjugate was then lyophilized (Sanyo ultra freeze, Japan). The developed nanoconjugate was characterized by Fourier-Transform infra-red (FT-IR) spectroscopy (Perkin Elmer 783, Pyrogen 1000 Spectrophotometer, USA) using KBR pellet method (Fig. 1) and scanned in the range from 4,000 to 500 cm^{-1}, and transmission electron microscopy (TEM; Morgani 268 D, Holland) after drying on carbon-coated copper grid and staining negatively by 1% PTA by metal shadowing technique (Fig. 2) (19,23,24).

Drug Loading in Functionalized MWCNTs

The loading of SSZ in to the functionalized MWCNTs was performed using the equilibrium dialysis membrane method

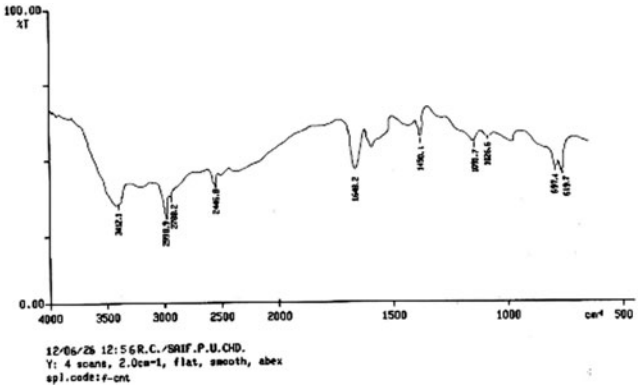

Fig. 1 FTIR spectrum of FUCO-MWCNTs.

(22–24,29). For this, functionalized MWCNTs (1 min sonicated) and SSZ in equal ratio of 1:1 were taken in PBS (pH 7.4) and incubated for 24 h with continuous magnetic stirring at 50 rpm . The content was then dialyzed using dialysis tubing (MWCO 12–14 KDa) against PBS (pH 7.4) under strict sink condition for 30 min to remove unentrapped SSZ. Amount of entrapped drug was determined by estimating the amount of free SSZ spectrophometrically at absorbance λ_{max} 359 nm (UV-1601, Shimadzu, Kyoto, Japan). The dialyzed formulation was filtered and used for further characterization. Similar procedure was adopted for the loading of SSZ in FUCO-MWCNTs and coded as SSZ loaded amine terminated (SSZ-MWCNTs) and SSZ loaded fucosylated MWCNTs (SSZ-FUCO-MWCNTs). The percent entrapment efficiency of MWCNTs formulations was calculated using the following equation (Fig. 3):

$$\%\ \text{Entrapment Efficiency(EE \%)} = \frac{\text{Weight of entrapped drug}}{\text{Weight of entrapped drug} + \text{free drug}} \times 100$$

Fig. 2 TEM image of FUCO-MWCNTs.

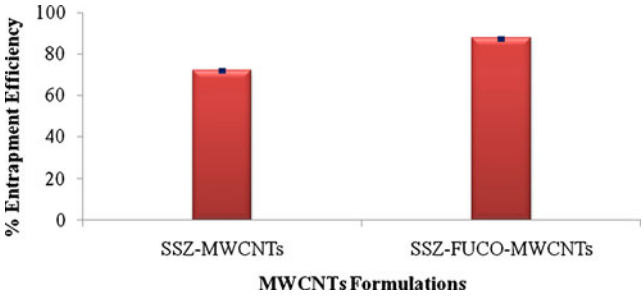

Fig. 3 The % entrapment efficiency of MWCNTs formulations (Mean ± S.D.; $n = 3$).

In Vitro Studies

In Vitro Drug Release

The known amounts of SSZ loaded amine terminated MWCNTs (SSZ-MWCNTs) and SSZ loaded fucosylated MWCNTs (SSZ-FUCO-MWCNTs) were taken in dialysis tubing (MWCO 6 kDa) and placed in 100 mL of PBS (pH 7.4) and acetate buffer (pH 4.0) separately at 37±0.5°C with slow magnetic stirring under strict sink conditions. Samples (1 mL) were withdrawn at predetermined time intervals and the volume of recipient compartment was replenished with equal volume of fresh medium, after each withdrawal. The drug concentration was determined in triplicate after appropriate dilution of aliquots, spectrophotometrically at λ_{max} 236 nm (for recipient medium-PBS pH 4.0) and at λ_{max} 359 nm (for recipient medium PBS pH 7.4) against the similar blank medium (23,24) (Fig. 4).

Stability Studies

SSZ loaded MWCNTs formulations SSZ-MWCNTs and SSZ-FUCO-MWCNTs were stored under dark (amber colour vials) and light (colourless vials) at 4±0.5°C, 25±0.5°C and 50±0.5°C in a stability chamber (REMI CHM-6S, Mumbai, India) for a period of 5 weeks. The samples were monitored initially and weekly up-to 5 weeks for any sign of precipitation, turbidity, crystallization, change in color, consistency and drug leakage. The data obtained was used for the analysis of any physical or chemical degradation at storage conditions and for determining the precaution(s) required for storage. Drug leakage was determined by monitoring the release of drug from the formulations after storage at different conditions (4±0.5°C, 25±0.5°C and 50±0.5°C). The formulation samples (2 mL) were dialyzed through a dialysis tubing (MWCO 6 KDa, Sigma) against external medium (100 mL of PBS pH 7.4) and analyzed for content of drug (SSZ) spectrophotometrically at λ_{max} 359 nm. The procedure was repeated weekly up-to 5 weeks. The percentage increase in drug release from the formulations was used to analyze the effect of accelerated condition of storage on the formulations (24,30).

Ex Vivo Studies

Hemolytic Toxicity

The hemolytic toxicity was performed following the reported procedure from our laboratory, with minor modifications (23,24,31–34). Human venous blood was collected in Hi-Anticlot blood collection vials (HiMedia Lab. Mumbai, India). The RBCs were separated from the whole blood by centrifugation (Remi, Mumbai, India) at 3,000 rpm for 5 min. Supernatant was collected and suspended in normal saline solution to get 10% hematocrit value. Then, 0.5 mL of suitably diluted free SSZ, raw MWCNTs, SSZ-MWCNTs and SSZ-FUCO-MWCNTs were added to 4.5 mL of normal saline and incubated for 1 h with RBCs suspension. After centrifugation, supernatants were diluted with an equal volume of normal saline and absorbance was measured at 540 nm in a spectrophotometer (UV/Vis, Shimadzu, 1601, Kyoto, Japan). RBCs suspension was added to 5 mL of 0.9%w/v NaCl solution (normal saline) and 5 mL distilled water, respectively to obtain 0% and 100% hemolysis. The degree of hemolysis was determined (Fig. 5) using the following equation:

$$\text{Hemolysis}(\%) = \frac{\text{Abs} - \text{Abs}_0}{\text{Abs}_{100} - \text{Abs}_0} \times 100$$

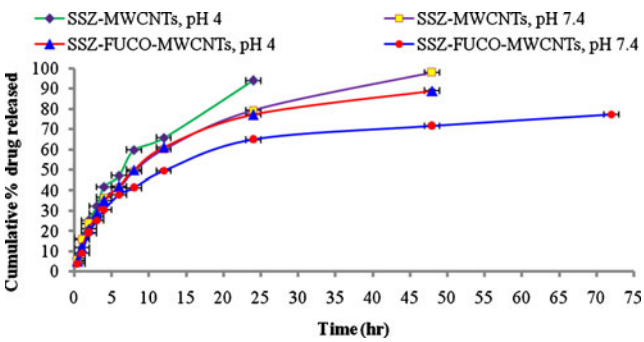

Fig. 4 Cumulative % drug release from MWCNTs formulations (Mean ± S.D.; $n = 3$).

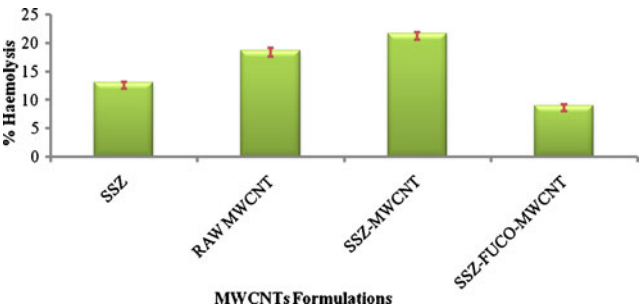

Fig. 5 % Hemolysis by free SSZ and MWCNTs formulations (Mean ± S.D.; $n = 3$).

where, Abs, Abs_{100} and Abs_0 are the absorbance of sample, a solution of 100% and 0% hemolysis, respectively.

Cell Culture

The J 774 macrophages cell line was maintained in fresh RPMI 1640 culture medium (HiMedia, Mumbai, India) supplemented with penicillin 10 U/mL; 10% fetal bovine serum (FBS); streptomycin 100 µg/mL; 1 mM sodium pyruvated and 10 mM HEPES medium; and transferred into a tissue culture plate with 96 wells and incubated for 48 h at 37±0.5°C in a humidified incubator (Digi Therm 2-CO_2, USA) with 5% CO_2 and 95% humidified atmosphere to acquire more than 75% confluency (23,28,35).

Cytotoxicity Studies (SRB Assay)

Cytotoxicity of developed nanotubes formulations was assessed *via* sulphorhodamine B (SRB) assay. This assay relies on the uptake of the anionic pink amino-xanthine dye, 'SRB' by basic amino acids where it forms an electrostatic complex with the basic amino acid residues of proteins under moderately acidic conditions. The greater the number of cells, the greater amount of dye is taken up and, after fixing, when the cells are lysed, the released dye will give a more intense color and greater absorbance. The 100 µL of each formulation (raw MWCNTs, SSZ-MWCNTs and SSZ-FUCO-MWCNTs) to be tested was taken in culture medium by adding into the 96-well plates containing the J774 macrophage cells (1×10^3cells in each well) in 1–1,000 µM concentration for 24 h. The cells were fixed with ice-cold trichloro acetic acid (TCA) for 1 h at 4°C. Culture plates were washed with distilled water five times and allowed to dry in the air. Fifty µL sulphorhodamine B (SRB) solution was added in to each well and allowed staining at room temperature for 30 min. SRB solution was removed by washing the plates quickly with 1%*v*/*v* acetic acid, five times, to remove unbound dye. Washed plates were dried in the air. The bound SRB was solubilized by adding 100 µL of 10 mM unbuffered Tris Base (pH 10.5) to each well and shaking for 5 min on a shaker platform. Plates were read in a 96-well plate reader at 492 nm (36,37). Cells devoid of any sample were used as control. The experiment was repeated three times for each sample. Cell viability of each group was compared with control and was expressed as % cell viability (Fig. 6) using following formula:

$$\text{Cell viability}(\%) = \frac{[A]_{\text{tested}}}{[A]_{\text{control}}} \times 100$$

where A_{treated} is the absorbance of treated cells with various samples, and A_{control} is the absorbance of control at 492 nm.

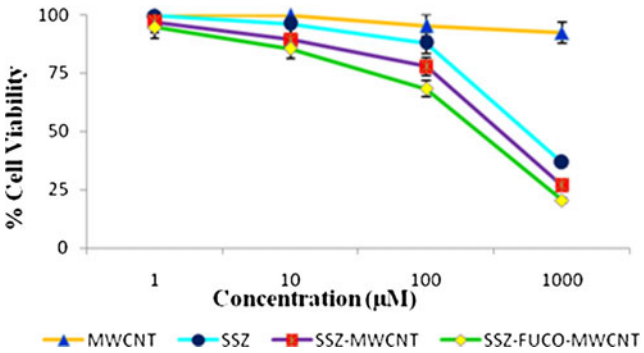

Fig. 6 % Cell viability of MWCNTs formulations. (Values represented as Mean ± S.D.; $n=3$).

Macrophage Uptake Assay

The cellular uptake efficiency as a function of conjugation of macromolecules was determined by incubation of macrophage cells with FITC loaded fucosylated as well as uncojugated MWCNTs using J774 macrophage cell lines. Uptake was performed at 1 and 6 h time interval. The dye fluorescein isothiocyanate (FITC) was loaded in MWCNTs formulations according to a reported method. SSZ-MWCNTs and SSZ-FUCO-MWCNTs were loaded with FITC by incubating MWCNTs (5 mg) formulations with 5 mL of 0.03*w*/*v*% FITC solution for 24 h, with intermittent shaking (23).

Ten µL of various FITC loaded formulations SSZ-MWCNTs and SSZ-FUCO-MWCNTs were suspended in the wells containing J774 macrophage cells. After incubation for 1 and 6 h cell lines were detached by pipetting and collected by centrifugation at 5,000 rpm for 2 min to remove nanocarriers adhering to cell surface. Cells were washed 5 times with PBS. Cell associated fluorescence was measured by fluorescence activated cell sorter (FACS) instrument ("BD" Bioscience, FACS Aria, Germany) using ~480 nm excitation, ~520 nm emission and the appropriate sensitivity settings (38) and macrophage uptake efficiency is shown in terms of intensity of fluorescence (Fig. 7).

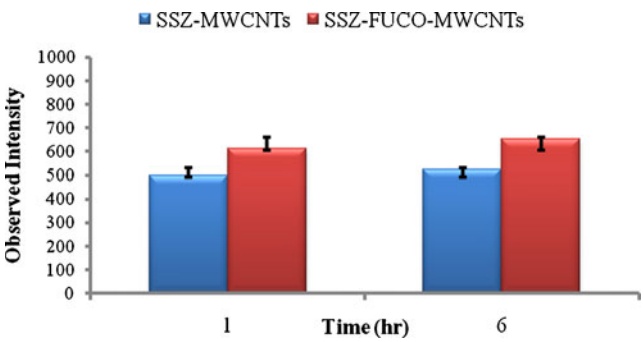

Fig. 7 Macrophage uptake of FITC loaded MWCNTs formulations. (Values represented as Mean ± S.D.; $n=3$).

NF-κB Inhibition Study

Cytokine Assay (Measurement of Inhibition in Interleukine-12 Level)

Ten µg/mL of lipopolysaccharides (LPs) was introduced in 96 wells plate containing J 774 macrophage cells in the absence (control) and presence of samples to be tested (free SSZ, SSZ-MWCNTs and SSZ-FUCO-MWCNTs). Cells were incubated for 48 h to ensure stimulation of the cells in case of control (stimulated cells produce higher amount of IL-12, which is the indication of NF-κB activation) and *vice versa* in case of samples. Culture supernatant was harvested and cytokine (IL-12p40) concentrations in the supernatants were determined by Enzyme Linked Immunosorbent Assay (ELISA) (39). Results obtained represent % inhibition in IL-12 (IL-12 p40) at different concentrations (Fig. 8).

Western Blot Analysis

Ten µg/mL of LPs was introduced in 96 wells plates containing macrophage cells in the absence (control) and presence of samples to be tested (free SSZ, SSZ-MWCNTs and SSZ-FUCO-MWCNTs). Cells were incubated for 48 h (40). Cells were washed with PBS and subsequently lysed in 25 mM Tris HCl, pH 7.5, 1 mM EDTA, 0.25 mM dithioerythritol, 0.1 M KCl, 1% Nonidet P40 (NP40), "complete" protease inhibitor cocktail (Boehringer Mannheim) and phosphatase inhibitor. The cell lysate was transferred to Eppendorf tubes, ultracentrifuged at 15,000 g (Z36HK, HERMLE LaborTchnik GmbH, Germany) and the supernatant was recovered. Cell extracts were analyzed according to standard protocols. Blots were pretreated in blocking buffer (5% of BSA) and subsequently incubated with anti p-IκB antibody. Bands were detected using the Western blotting detection reagent (41) (Fig. 9).

In Vivo Studies

The *in-vivo* studies were carried out on 8 weeks old male albino rats (Sprague–Dawley, 150±20 g). The experimental protocol was duly approved by the Committee for the Purpose of Control and Supervision of Experiments on Animals (CPCSEA) of Dr. H.S. Gour University, Sagar, M.P., India (CPCSEA letter number: Animal Eths. Committe/12/439/2012). For *in vivo* studies drug concentrations in blood samples and organ homogenates were determined by HPLC method (Shimadzu, C18, Japan) using mobile phase (methanol: acetonitrile : water; 35:35:30*v*/*v*) at 1 mL/min flow rate by C18-RP column (42).

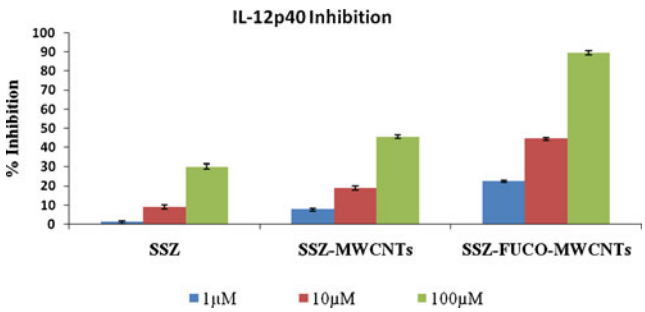

Fig. 8 % Inhibition of IL-12 (IL-12p40) level in macrophage cell line J774 by MWCNTs formulations and free SSZ.

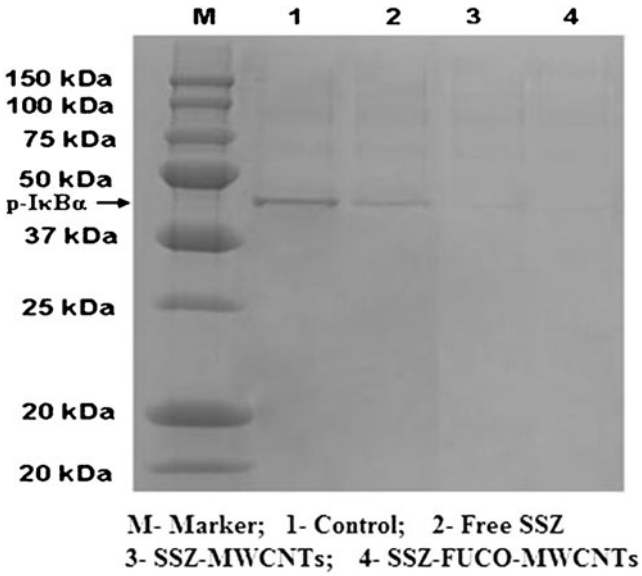

Fig. 9 Determination of phosphorylated-IκB (p-IκBα) protein in LPS activated macrophage cell by Western blot analysis.

Blood Level Studies

The blood level study was performed following the previously reported method from our laboratory (32,33,43), with slight modification. The animals were divided in to three groups each comprising of 3 rats and marked adequately. Animals were fasted overnight prior to administration of formulations. Formulations (SSZ-MWCNTs and SSZ-FUCO-MWCNTs) and the free SSZ solubilized in PBS (pH 7.4) (suspended in case of free SSZ) in the dosage of 20 mg/kg body weight were administered intravenously to each rat of the first, second, and third group, respectively *via* caudal vein. One rat from each group was sequentially taken and 0.2 mL of blood was withdrawn from retro-orbital plexus in Hi-Anticlot vials (HiMedia, Mumbai, India) after 0.5, 1.0, 2.0, 3.0, 4.0, 6.0, 8.0, 12.0, 18.0, 24.0, 30.0 and 36.0 h time intervals from each group. In each case blood was centrifuged at 3,000 rpm (REMI, Mumbai, India) for 10 min. The upper supernatant (plasma) was collected separately with the help of micropipette, 100 µL of acetonitrile was added to the 100 µL of sample and the contents were vortexed (Superfit vortexer, India) for 1 min and 5 mL methanol was added to it. The mixture was extracted for 10 min and centrifuged at 3,000 rpm for 10 min. The supernatant was decanted into another vial and evaporated to dryness at 60°C. The dried residue was

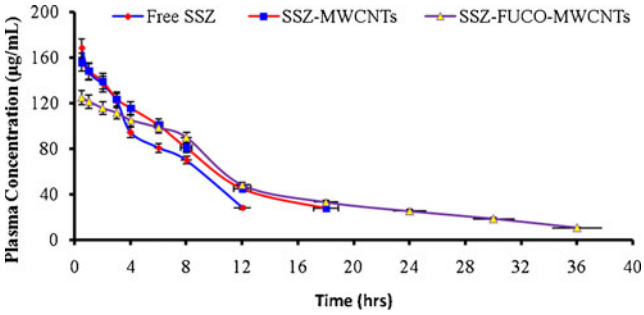

Fig. 10 Comparative plasma drug concentration profile of MWCNTs formulations and free SSZ. Values represented as Mean ± SD ($n = 3$).

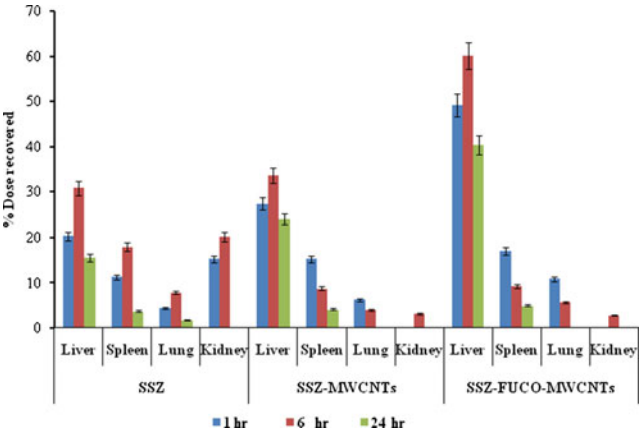

Fig. 11 SSZ levels attained in different organs after administration of free SSZ and MWCNTs formulations. Values represented as Mean ± SD ($n = 3$).

reconstituted with 1 mL methanol and ultra-centrifuged at 15,000 rpm (Z36HK, HERMLE LaborTchnik GmbH, Germany) for 10 min. Clear supernatant was collected and amount of SSZ was determined (Fig. 10) by HPLC method (42) and various pharmacokinetic parameters (C_{max}, K_{el}, $t_{1/2}$, AUC, AUMC and MRT) were calculated using Kinetica 5 PK/PD, Thermo Scientific, USA software (Table I).

Biodistribution Studies

Tissue distribution studies were carried out for quantitative measurement of SSZ in different organs. Rats were divided into three groups, each group comprising 9 animals ($n = 3$). Animals were fasted overnight before administration of dose. To the first group plain drug solution (20 mg/kg) in PBS (pH 7.4); to the second and third groups SSZ-MWCNTs and SSZ-FUCO-MWCNTs, respectively were administered through the caudal vein. After 1, 6 and 24 h three animals from each group were sacrificed. The organs (spleen, kidney, liver, and lungs) were excised and homogenized. The homogenates were deproteinized with acetonitrile, centrifuged, filtered and estimated for the drug contents by HPLC method (42). The results are expressed as percentage dose recovered from each organ (Fig. 11).

Hematological Studies

Hematological parameters were estimated following to the earlier reported method (32,33,43,44). Animals were divided into six groups comprised of three rats in each group. Animals of group-1 were kept as control. All animals were fasted overnight before administration of dose. Animals of group 2, 3 and 4 were administered with free drug (SSZ), SSZ-MWCNTs and SSZ-FUCO-MWCNTs, respectively in a dose of 20 mg/kg body weight intravenously everyday up to 7 days. Animals were maintained on same regular diet upto 7 days. After 7 days blood samples were collected from the animals and analyzed for red blood corpuscles (RBCs), white blood corpuscles (WBCs) and differential count of monocytes, lymphocytes and neutrophils, % Hb, MCH and HCT (Table II).

Statistical Analysis

The results are expressed as mean ± standard deviation (mean ± S.D.) and statistical analysis was performed with Graph Pad Instat Software (Version 3.00, Graph Pad Software, San Diego, California, USA) by analysis of variance (ANOVA) followed by Tukey–Kramer multiple comparison test. A probability of $p \leq 0.05$ was considered statistically significant. Pharmacokinetic parameters were calculated using the Kinetica 5 PK/PD software (Thermo Scientific, USA).

Table I Pharmacokinetic Parameters of Free SSZ, SSZ-MWCNTs, and SSZ-FUCO-MWCNTs

Parameters Formulations	C_{max} (µg/mL)	$AUC_{(0-\infty)}$ (µg.hr/mL)	$AUMC_{(0-\infty)}$ (µg.hr^2/mL)	$t_{1/2}$ (hr)	Kel (hr^{-1})	MRT (hr)
Free SSZ	168.01 ± 0.93	1004.55	7337.83	5.06	0.14	7.30
SSZ-MWCNTs	155.62 ± 0.61	1262.47	11529.38	6.33	0.11	9.13
SSZ-FUCO-MWCNTs	124.80 ± 0.74	1646.99	23595.76	9.92	0.07	14.33

Values Represented as Mean ± SD ($n = 3$)

MRT Mean Residence Time; C_{max} Maximum Plasma Concentration; $t_{1/2}$ Half life; K_{el} Elimination constant; *AUC* Area Under Curve

Table II Hematological Parameters of Albino Rats Treated with SSZ and SSZ Loaded Formulations

S.No.	Formulations	Hematological parameters							
		RBCs count (× $10^6/\mu L$)	WBC COUNT (× $10^3/\mu L$)	Differential counts (× $10^3/\mu L$)			Hb (g/dL)	MCH (pg)	HCT %
				Monocytes	Lymphocytes	Neutrophils			
1	Control	9.1 ± 0.10	10.30 ± 0.44	1.69 ± 0.12	7.71 ± 0.55	1.47 ± 0.15	13.09 ± 0.69	18.41 ± 0.42	43.59 ± 0.66
2	Drug (SSZ)	7.70 ± 0.19	11.66 ± 0.42	1.57 ± 0.06	8.73 ± 0.15	1.77 ± 0.05	11.28 ± 0.39	16.23 ± 0.29	36.03 ± .80
5	SSZ-MWCNTs	5.33 ± 0.15	14.66 ± 0.76	1.60 ± 0.10	9.66 ± 0.70	2.47 ± 0.50	10.53 ± 0.45	15.23 ± 0.58	28.33 ± 1.5
6	SSZ-FUCO-MWCNTs	8.88 ± 0.31	10.6 ± 0.62	1.26 ± 0.30	8.86 ± 0.34	3.06 ± 0.31	12.03 ± 0.25	17.43 ± 0.40	42.17 ± 0.80

#Values represented as mean ± S. D. ($n = 3$)

RESULTS AND DISCUSSION

Initially, purification of the pristine MWCNTs was done using hot air oven and chemical treatment. After purification, functionalization was carried out on to disperse MWCNTs (as MWCNTs are insoluble in water and other aqueous media/solvents) and to conjugate ligand with them. Therefore, before Fucosylation, the first generation (pristine) MWCNTs was initially purified, carboxylated, acylated and amidated, and characterized. Till date there is no report on the fucose conjugation, characterization, and *in vitro- in vivo* evaluation of SSZ loaded fucosylated functionalized MWCNTs and in that sense this is a debut report using SSZ loaded fucose tethered surface modified MWCNTs.

Fucosylation of amine terminated MWCNTs was done by ring opening reaction followed by reaction of aldehyde groups of fucose with the amino groups of MWCNTs in 0.1 M sodium acetate buffer (pH 4.0) (19,23). This leads to the formation of Schiff's base (−N = CH−), which may possibly get reduced to secondary amine (−NH−CH_2−) but stay in equilibrium with Schiff's base (Scheme 2). FTIR analysis proved the formation of Schiff's base and secondary amine (−NH−CH_2−) linkage between aldehyde groups of fucose and end terminal amine functional groups of functionalized MWCNTs (Fig. 1).

The electron microscopy of the FUCO-MWCNTs was carried out to determine the surface topography and Fig. 2 clearly depict in nanometric size range with tubular structure. The surface charge and average particle size were determined by photon correlation spectroscopy in a Malvern Zetasizer nano ZS90 (Malvern Instrument Ltd, Malvern, UK) at room temperature (RT). The fucosylated MWCNTs showed the zeta potential and average particle size +4.5 mV at neutral pH and 150 ± 1.6 nm.

The physical binding of drug molecules inside as well as on the nanotubes surface is ascribed to the non-covalent interactions such as hydrophobic interaction (45) and hydrogen bonding (40) among SSZ and FUCO-MWCNTs. The percentage drug loading was determined indirectly by estimating the un-entrapped drug spectrophotometrically. The MWCNTs and FUCO-MWCNTs showed 72.15 ± 0.14% and 87.77 ± 0.11% SSZ loading, respectively (Fig. 3). The percentage SSZ loading of FUCO-MWCNTs was significantly increased compared to MWCNTs. The increased loading was possibly due to the π-π stacking, electrostatic, and adsorption interactions between SSZ and FUCO-MWCNTs. Higher entrapment efficiency of SSZ in FUCO-MWCNTs was due to the availability of greater surface area for π-π stacking, adsorption and electrostatic interaction as compared to bundled amine terminated MWCNTs (46). Our results are in agreement with the previous reports (21–24,29).

Cumulative release of SSZ from SSZ-MWCNTs and SSZ-FUCO-MWCNTs formulations was dependent on the pH of the micro-environment. The rate of drug release from the formulations at pH 4.0 and 7.4 suggested the sustained release pattern (Fig. 4). The release studies suggested that both SSZ-MWCNTs and SSZ-FUCO-MWCNTs showed initial burst release of SSZ at pH 4.0. The drug release was found to be 94.10 ± 0.15% for SSZ-MWCNTs at 24th hr and 89.12 ± 0.71% for SSZ-FUCO-MWCNTs at 48th hr. On the contrary SSZ release was significantly ($P \leq 0.05$) retarded from SSZ-FUCO-MWCNTs at pH 7.4 (64.89 ± 0.87% at 24th hr) as compared to SSZ-MWCNTs (79.47 ± 0.25% at 24th hr). SSZ-FUCO-MWCNTs nano-carrier released 77.45 ± 0.21 of SSZ up to 72th hr. The π-π stacking interactions at pH 7.4 are easily broken down at acidic microenvironment and release the drug molecules. The results of our *in vitro* release studies are in line with the previous reports (22–24,29,47).

The stability study is an important parameter prior to the development of safer nanomedicines as per the Food and Drug Administration (FDA) guidelines (48). The stability data of SSZ-MWCNTs and SSZ-FUCO-MWCNTs was evaluated at various conditions of temperature (4 ± 0.5, 25 ± 0.5 and 50 ± 0.5°C) after keeping in dark (amber color glass vials) as well as in light (colorless vials) for a period of 5 weeks. The formulation was found to be the most stable in dark at 4 ± 0.5°C storage condition. In terms of stability profile of

various nano-range delivery modules, MWCNTs could possibly present themselves as a most stable system in all temperature ranges and environment required for biological applications (49). The drug leakage was found to be minimum at room temperature as compared to that at 4±0.5°C, which may be due to the shrinking of the MWCNTs architecture leading to decrease in cavity enclosing drug molecules. Leakage of drug from the SSZ-FUCO-MWCNTs was found to be greater at higher temperature (50±0.5°C). However, the possible reason behind such variable release could not be explored. At higher temperature fucose molecules gain higher kinetic energy and as a result ring is wide open and the fucose molecules that shield the cavities spread in the medium. The drug leakage was found to be more in formulations stored in light than those kept in dark. This may be attributed to structure cleavage at higher temperature and light leading to bond breakage due to higher reaction kinetics. From above, it can be concluded that the SSZ-FUCO-MWCNTs are more stable in dark and at 4 than at 25, 50±0.5°C (24).

The free SSZ showed 13.01±0.13% hemolysis, whereas raw MWCNTs produced 18.64±0.51% hemolysis (Fig. 5). Although the hemolytic toxicity of SSZ-MWCNTs was found to be 21.62±0.24% yet, the hemolytic toxicity of SSZ-FUCO-MWCNTs was drastically reduced to 9.01±0.23% ($p \leq 0.05$) (Fig. 5). Fucose attachment considerably reduced the hemolysis of RBCs possibly due to shielding of the terminal -NH_2 groups responsible for hemolysis. However the probable reason could be that the surface functionalization dramatically reduce the erythrocytes toxicity and renders it suitable for drug delivery without any toxic effects. In this way interaction of cell membranes of RBCs with cationic terminals of amine terminated MWCNTs is prevented and hence less hemolysis occurs. The obtained results are in accordance with the previous reports (23,24).

In vitro cytotoxicity assay was carried out on *J774* cells *via* SRB assay by incubating different formulations for 24 h. Unloaded raw MWCNTs did not shown any significant cytotoxicity effect after 24 h incubation even at higher concentration (100 μM). SSZ exerted dose dependent cytotoxicity (Fig. 6). Free SSZ showed negligible cytotoxicity upto 100 μM, however above 100 μM it showed significant cytotoxicity (% cell viability <40). The higher cytotoxicity of SSZ-MWCNTs than free SSZ might be due to higher interaction of positively charged amino terminated MWCNTs with negatively charged cell membranes. SSZ-FUCO-MWCNTs showed more cytotoxicity than raw MWCNTs, SSZ-MWCNTs and free SSZ. The fucosylation of MWCNTs might have contributed to higher cytotoxicity of SSZ-FUCO-MWCNTs due to more accumulation of SSZ inside the cell *via* receptor mediated endocytosis (RME). However, our aim was not to kill macrophages but to detect that the dose selected for the treatment of disease, is not cytotoxic to the cells and the data revealed that the dose selected was non-cytotoxic to macrophages. Results of macrophage uptake assay revealed that with the increase of time, mean FITC measured intensity was found to be increased in macrophage cell line (J774), which may be due to more cellular uptake of FITC loaded fucosylated MWCNTs than unconjugated MWCNTs formulations (Fig. 7). This may be due to lack of receptor-ligand interaction in case of unconjugated MWCNTs.

Results of cytokine assay show that the incubation of J774 cells with LPS (10 μg/mL) for 48 h caused the appearance of IL-12 p40 in the culture supernatants. However, treatment of the cells with sulfasalazine (SSZ) and various nanotubes formulations suppressed *IL*-12 p40 production in a dose-dependent manner (39). On comparing MWCNTs formulations; more significant % inhibition was observed with SSZ-FUCO-MWCNTs as compared to SSZ-MWCNTs and free SSZ (Fig. 8) that could be ascribed to the higher cellular uptake due to the receptor-mediated internalization of SSZ-FUCO-MWCNTs.

Upon NF-κB activation, IκB protein phosphorylates, thus the presence of phosphorylated-IκB (p-IκB) in cell lysates of J774 cells is the indication of NF-κB activation (Fig. 9). Western blot analysis showed a clear band (between 50 and 37 KDa) of p-IκB with control (J774 cells incubated with LPS only). Chen *et al.* also reported the band of p-IκB between 46 and 30 KDa in western blot analysis (50). However band intensities were found to be decreased when cells were treated with SSZ and SSZ loaded MWCNTs. Reason of decreased band intensities is possibly the inhibition of NF-κB activation. Hence there was less or no production of p-IκB, thus no band was observed when cells were treated with SSZ-FUCO-MWCNTs. Disappearance of band suggested the complete inhibition of NF-κB activation.

The blood level study was carried out following *i.v.* administration of developed formulations to study the effect of presence of macromolecules on the release profile and retention of MWCNTs formulations in systemic circulation. The drug concentration in blood plasma samples was determined at various time intervals. The release of formulations was found to be sustained *in-vivo* also (Fig. 10). The pharmacokinetic data shows that the formulation had a slightly lower C_{max} (124.80±0.74 μg/mL in case of SSZ-FUCO-MWCNTs formulations) as compared to free SSZ (168.01±0.93 μg/mL) (Table I). However, the duration of drug concentration in blood *via* formulations was prolonged *i.e.* from 12 h to 36 h in case of SSZ-FUCO-MWCNTs. The plasma drug concentration with the free drug was detected till 12th hr and that too in trace quantities, and thereafter no drug was detected suggesting its metabolism *via* liver and subsequent excretion. The mean residence time (MRT) of the formulation 14.33 h in case of SSZ-FUCO-MWCNTs formulations was found to be increased significantly in comparison to free SSZ (7.30 h). The MRT of SSZ-FUCO-

MWCNTs (14.33 h) was approximately two folds higher in comparison to free SSZ (7.30 h). The area under the mean curve ($AUMC_{0-\infty}$) of the SSZ-FUCO-MWCNTs formulation was found about three folds (23595.76 μg.hr^2/mL) higher to the free SSZ (7337.83 μg.hr^2/mL) owing to the surface modification of nanotubes as revealed from the Table I. This indicates that the metabolism (and hence excretion) has been escaped in significant manner by entrapping SSZ in the SSZ-FUCO-MWCNTs systems as compared to the free SSZ. The plasma concentration *vs.* time curve also reveals an increased residence time of SSZ-MWCNTs formulations (9.13 h) and the reason for this may be the same as for the SSZ-FUCO-MWCNTs. The pharmacokinetic data of surface modified fucosylated MWCNTs clearly indicated that the degree of functionalization increased the kinetic parameters beneficially in development of safe and effective nanomedicines.

Biodistribution study was performed to evaluate targeting efficiency of SSZ from different formulation. The concentration of SSZ in different organs was estimated *via* HPLC (42) at 1st, 6th and 24th hr. The results indicated that the free SSZ accumulated progressively in liver, where up to 30.25±0.56% of dose is localized after 1 h of administration but after 24 h only 4.54±0.12% and 2.70±0.19% of SSZ was found in liver and spleen respectively (Fig. 11). The amount of SZZ in body depends upon its distribution, metabolism and excretion. Initially, the free SSZ content in liver was highest but declined consequently in case of free SSZ formulation. This might be due to rapid elimination of SSZ from liver, the prime site of its action. In case of SSZ-MWCNTs, drug was found to be primarily accumulated in liver and spleen but the drug release was not sustained as the amount of drug in liver was reduced from 27.36±0.71% (at 1 h) to 24.04±0.67% (at 24 h). The drug was found to be rapidly excreted through the kidney. Thus high uptake of formulations in macrophage rich organs was due to the RES uptake. But in case of SSZ-FUCO-MWCNTs, the drug was primarily found to be accumulated in liver and spleen that may be due to the receptor-mediated endocytotic uptake of fucosylated MWCNTs formulations by macrophages (Fig. 11). In this case, the drug in liver at first hr was found to be 49.19±0.88% of initial dose, which was increased upto 60.12±0.96% for SSZ-FUCO-MWCNTs. At 24 h the drug in liver was found to be 40.31±0.79% of initial dose. In spleen, the drug at first hr was found to be 16.89±0.51% of initial dose At 24 h the drug in spleen was found to be 4.94±0.23% of initial dose. Comparing this data with that from free drug solution and SSZ-MWCNTs it is inferred that fucosylated MWCNTs was highly accumulated in macrophage rich organs and provided a sustained release of drug. Yeeprae *et al.* reported similar results of accumulation of mannosylated system in macrophage rich organs (51). Meng *et al.* investigated the immunological properties of modified (oxidised) water dispersible MWCNTs injected subcutaneously into healthy BALB/c mice. The authors indicated that the MWCNTS induces obvious short-term immunological reactions, which can be easily eliminated over-time (52). Jain *et al.* reported that the well-individualized MWCNTs with shorter lengths (less than 500 nm) and higher degree of oxidation (surface carboxyl density >3 μmol/mg) are not retained in any RES rich organs and rapidly cleared out from the systemic circulation (53).

The biodistribution studies clearly indicate the superiority of the SSZ-FUCO-MWCNTs, when compared against the plain drug towards increasing the accumulation of SSZ in the liver. The data can be well correlated for MWCNTs with the study, where, amphotericin B entrapped mannosylated-MWCNTs were used by Pruthi *et al.* for disposition of drug to liver only (23). Thus our results on biodistribution are in accordance with the previously published reports (23,52,53). Schipper *et al.* also previously reported that SWCNTs do not induce any obvious toxicity upon intravenous administration (54).

The hematological parameters RBCs, WBCs and differential lymphocytes count were evaluated to assess the relative effect of different drug loaded formulations as compared to the free SSZ. The RBCs count was found to be decreased below normal values more in case of SSZ-MWCNTS (5.33±0.15) than that of SSZ-FUCO-MWCNTs (8.88±0.31). This result is correlated to more hemolytic toxicity of SSZ-MWCNTs as compared to SSZ-FUCO-MWCNTs. The WBCs count of SSZ-MWCNTs (14.66±0.76) was found to increase significantly as compared to normal values however, for SSZ-FUCO-MWCNTs (10.6±0.62), the increase was less than that of un-conjugated formulation and even less than the normal count in controlled group (Table II). Similarly, a relative increase in lymphocyte and neutrophils count was observed with SSZ-MWCNTs but in case of SSZ-FUCO-MWCNTs, the increase was less. This could be attributed to the fact that due to the presence of polycationic charge, the cell cytotoxicity of SSZ-MWCNTs was increased and that could lead to increased level of lymphocytes as well as neutrophils. Levels of hemoglobin, MCH and %HCT were found to decrease more in case of unconjugated formulation than that of conjugated (fucosylated) formulations. Data obtained from this study can be well correlated with earlier reports (43,44,55).

CONCLUSION

It is concluded that surface modified MWCNTs having biocompatible framework exhibit reduced toxicity and at the same time exhibit a sustained drug release behavior *in vitro* as well as *in vivo* (18,20,22–24,29,56,57). SRB assay, macrophage uptake assay, fluorescence microscopy and biodistribution data demonstrated that fucosylated nanoconjugate has potential to deliver significantly higher amount of drug to liver for higher therapeutic outcome. The result of hemolytic toxicity and hematological studies revealed that fucose conjugation

can be utilized to reduce the toxicity associated with unconjugated MWCNTs. Cytokine assay also suggested that SSZ-FUCO-MWCNTs exhibits significantly higher inhibition of IL-12 p40 secretion. Western blot assay suggested that SSZ-FUCO-MWCNTs significantly inhibit NF-κB activation. Overall we can conclude that SSZ-FUCO-MWCNTs hold great potential as site-specific, targeted, safe, therapeutically more effective drug delivery for *i.v.* administration.

ACKNOWLEDGMENTS AND DISCLOSURES

Authors Richa Gupta and Neelesh Kumar Mehra are thankful to the University Grants Commission (UGC), New Delhi, India for providing the Junior Research Fellowship (JRF) to during the tenure of the studies. The authors report no conflict of interest.

REFERENCES

1. Nishikori M. Classical and alternative NF-κB activation pathways and their roles in lymphoid malignancies. J Clin Exp Hematopathol. 2005;45(1):15–24.
2. Tak PP, Firestein GS. NF-κB: a key role in inflammatory diseases. J Clin Investig. 2001;107(1):7–11.
3. Robinson SM, Man DA. Role of nuclear factor κB in liver health and disease. Clin Sci. 2010;118:691–705.
4. Tsukamoto H. Redox regulation of cytokine expression in Kupffer cells. Antioxid Redox Signal. 2002;4:741–8.
5. Decker K. Biologically active products of stimulated liver macrophages (Kupffer cells). Eur J Biochem. 1990;192:245–61.
6. Handa O, Naito Y, Takagi T, Shimozawa M, Kokura S, Yoshida N, *et al.* Tumor necrosis factor-alpha-induced cytokine-induced neutrophil chemoattractant-1 (CINC-1) production by rat gastric epithelial cells: role of reactive oxygen species and nuclear factor-kB. J Pharmacol Exp Ther. 2004;309:670–6.
7. Travis SPL, Jewell DP. Salicylates for ulcerative colitis-their mode of action. Pharmacol Ther. 1994;63:135–61.
8. Wahl C, Liptay S, Adler G, Schmid RM. Sulfasalazine: a potent and specific inhibitor of nuclear factor kappa B. J Clin Investig. 1998;101(5):1163–74.
9. D'Acquisto F, May MJ, Ghosh S. Inhibition of nuclear factor kappa B (NF-κB): an emerging theme in anti-inflammatory therapies. Mol Interv. 2002;2(1):22–35.
10. Schorder H, Campbell DES. Absorption, metabolism and excretion of salicylazosulfapyridine in man. Clin Pharmacol Ther. 1972;13:539–51.
11. Kawakami S, Wong J, Sato A, Hattori Y, Yamashita F, Hashida M. Biodistribution characteristics of mannosylated, fucosylated, and galactosylated liposomes in mice. Biochim Biophys Acta. 2002;1524:258–65.
12. Mehra NK, Jain AK, Lodhi N, Raj R, Dubey V, Mishra DK, *et al.* Challenges in the use of carbon nanotubes for biomedical applications. Crit Rev Ther Drug Carrier Syst. 2008;25(2):169–220.
13. Jain NK, Mishra V, Mehra NK. Targeted drug delivery to macrophages. Exp Opin Drug Deliv. 2013;10(3):353–67.
14. Jain AK, Mehra NK, Lodhi N, Dubey V, Mishra D, Jain NK. Carbon nanotubes and their toxicity. Nanotoxicol. 2007;1:167–97.
15. Mehra NK, Mishra V, Jain NK. Receptor-based targeting of therapeutics. Ther Deliv. 2013;4(3):369–94.
16. Kesharwani P, Ghanghoria R, Jain NK. Carbon nanotubes exploration in cancer cell lines. Drug Discov Today. 2012;17(17–18):1023–30.
17. Montes-Fonseca SL, Orrantia-Borunda E, Aguilar-Elguezabal A, Gonzalez Horta C, Talamas-Rohana P. Cytotoxicity of functionalized carbon nanotubes in J774A macrophages. Nanomed Nanotechnol Biol Med. 2012;8:853–9.
18. Meng L, Zhang X, Lu Q, Fei Z, Dyson PJ. Single walled carbon nanotubes as drug delivery vehicles: targeting doxorubicin to tumors. Biomaterials. 2012;33(6):1689–98.
19. Jain AK, Dubey V, Mehra NK, Lodhi N, Nahar M, Mishra DK, *et al.* Carbohydrate-conjugated multiwalled carbon nanotubes: development and characterization. Nanomed Nanotechnol Biol Med. 2009;5(4):432–42.
20. Lacerda L, Russier J, Pastorin G, Herrero MA, Venturelli E, Dumortier H, *et al.* Translocation mechanisms of chemically functionalized carbon nanotubes across plasma membranes. Biomaterials. 2012;33:3334–43.
21. Zhang X, Meng L, Lu Q, Fei Z, Dyson PJ. Targeted delivery and controlled release of doxorubicin to cancer cells using modified single wall carbon nanotubes. Biomaterials. 2009;30:6041–7.
22. Ji Z, Lin G, Lu Q, Meng L, Shen X, Dong L, *et al.* Targeted therapy of SMMC-7721 liver cancer in vitro and in vivo with carbon nanotubes based drug delivery system. J Colloid Interface Sci. 2012;365:143–9.
23. Pruthi J, Mehra NK, Jain NK. Macrophages targeting of amphotericin B through mannosylated multiwalled carbon nanotubes. J Drug Target. 2012;20(7):593–604.
24. Lodhi N, Mehra NK, Jain NK. Development and characterization of dexamethasone mesylate anchored on multi walled carbon nanotubes. J Drug Target. 2013;21(1):67–76.
25. Higuchi Y, Kawakami S, Yamashita F, Hashida M. The potential role of fucosylated cationic liposome/NF-κB decoy complexes in the treatment of cytokine-related liver disease. Biomaterials. 2007;28:532–9.
26. Zheng B, Li Y, Liu J. CVD synthesis and purification of single walled carbon nanotubes on aerogel-supported catalyst. Appl Phys A. 2002;74:345–8.
27. Li CC, Lin JC, Huang SJ, Lee JT, Chen CH. A new and acid exclusive method for dispersing multi-walled carbon nanotubes in aqueous suspensions. Colloids Surf A Physicochem Eng Asp. 2007;297:275–81.
28. Nahar M, Jain NK. Preparation, characterization and evaluation of targeting potential of amphotericin B-loaded engineered PLGA nanoparticles. Pharm Res. 2009;26:2588–98.
29. Ren J, Shen S, Wang D, Xi Z, Guo L, Pang Z, *et al.* The targeted delivery of anticancer drugs to brain glioma by PEGylated oxidised multi-walled carbon nanotubes modified with angiopep-2. Biomaterials. 2012;33:3324–33.
30. Bhadra D, Bhadra S, Jain S, Jain NK. A PEGylated dendritic nanoparticulate carrier of fluorouracil. Int J Pharm. 2003;57:111–24.
31. Jain V, Swarnakar NK, Mishra PR, Verma A, Kaul A, Mishra AK, *et al.* Paclitaxel loaded PEGylated glyceryl monooleate based nanoparticulate carriers in chemotherapy. Biomaterials. 2012;33(29):7206–20.
32. Agrawal A, Gupta U, Asthana A, Jain NK. Dextran conjugated dendrite nanoconstructs as potential vectors for anti-cancer agent. Biomaterials. 2009;30:3588–96.
33. Gajbhiye V, Jain NK. The treatment of Glioblastom a xenografts by surfactant conjugated de ndritic nanoconjugates. Biomaterials. 2011;32(26):6213–25.
34. Patel SK, Gajbhiye V, Jain NK. Synthesis, characterization and brain targeting potential of paclitaxel loaded thiamine-PPI nanoconjugates. J Drug Target. 2012;20(10):841–9.
35. Duverger A, Jackson RJ, Van Ginkel FW, Fischer R, Tafaro A, Leppla SH, *et al.* Bacillus anthracis edema toxin acts as an adjuvant for mucosal immune responses to nasally administered vaccine antigens. J Immunol. 2006;176(3):1776–83.

36. Houghton P, Fang R, Techatanawat I, Steventon G, Hylands PJ, Lee CC. The sulphorhodamine (SRB) assay and other approaches to testing plant extracts and derived compounds for activities related to reputed anticancer activity. Methods. 2007;42:377–87.
37. Perez RP, Godwin A, Handel LM, Hamilton TC. A comparison of clonogenic, microtetrazolium and sulforhodamine B assays for determination of cisplatin cytotoxicity in human ovarian carcinoma cell lines. Eur J Cancer. 1993;29A(3):395–9.
38. Singodia D, Verma A, Verma RK, Mishra PR. Investigations on alternate approach to target mannose receptors on macrophages using 4-sulfated n-acetyl galactosamine more efficiently as compared to mannose decorated liposomes: an application in drug delivery. Nanomed Nanotechnol Biol Med. 2012;8(4):468–77.
39. Haskoa G, Szaboa C, Neameth ZH, Deitch EA. Sulphasalazine inhibits macrophage activation: inhibitory effects on inducible nitric oxide synthase expression, interleukin-12 production and major histocompatibility complex II expression. Immunology. 2001;103:473–8.
40. Newkome GR, Woosley BD, He E, Moorefield CN, Guther R, Baker GR, *et al*. Supramolecular chemistry of flexible, dendritic based structures employing molecular recognition. Chem Commun. 1996;24:2737–8.
41. Rodenburg RJT, Ganga A, Van Lent PLEM, Van De Putte LBA, Van Venrooij WJV. The antiinflammatory drug sulfasalazine inhibits tumor necrosis factor α expression in macrophages by inducing apoptosis. Arthritis Rheum. 2000;43(9):1941–50.
42. Jianquin C. Determination of sulfasalazine tablets by HPLC. Chin Pharm Aff. 2007;08–13.
43. Agrawal P, Gupta U, Jain NK. Glycoconjugated peptide dendrimers-based nanoparticulate system for the delivery of chloroquine phosphate. Biomaterials. 2007;28:3349–59.
44. Gupta U, Dwivedi SK, Bid HK, Konwar R, Jain NK. Ligand anchored dendrimers based nanoconstructs for effective targeting to cancer cells. Int J Pharm. 2010;393(1–2):185–96.
45. Newkome GR, Moorefield CN, Baker GR, Saunders MJ, Grossman SH. Unimolekulare micellen. Angew Chem Int Ed. 1991;103:1207–9.
46. More N, Vander Kolk JV, Heifets I. Accumulation of clarithromycin in macrophages infected with M. avium. Pharmacol Ther. 1994;14:100–4.
47. Gu YJ, Cheng J, Jin J, Cheng SH, Wong WT. Development and evaluation of pH-responsive single-walled carbon nanotube-doxorubicin complexes in cancer cells. Int J Nanomedicine. 2011;6:2889–98.
48. Bawa R. Regulating nanomedicines-can the FDA handle it? Curr Drug Deliv. 2011;8(3):227–34.
49. Wang Y, Iqbal Z, Malhotra SV. Functionalization of carbon nanotubes with amines and enzymes. Chem Phys Lett. 2005;402(1–3):96–101.
50. Chen Z, Hagler J, Palombella VJ, Melandri F, Seherer D, Ballard D, *et al*. Signal-induced site-specific phosphorylation targets IκBα to the ubiquitin-proteasome pathway. Genes Dev. 1995;9:1586–97.
51. Yeeprae W, Kawakami S, Yamashita F, Hashida M. Effect of mannose density on mannose receptor-mediated cellular uptake of mannosylated O/W emulsions by macrophages. J Control Release. 2006;114(2):193–201.
52. Meng J, Yang M, Jia F, Xu Z, Kong H, Xu H. Immune response of BALB/c mice to subcutaneously injected multi-walled carbon nanotubes. Nanotoxicol. 2010;5(4):583–9.
53. Jain S, Thakare VS, Das M, Godugu C, Jain AK, Mathur R, *et al*. Toxicity of multi walled carbon nanotubes with end defects critically depends on their functionalization density. Chem Res Toxicol. 2011;24(11):2028–39.
54. Schipper ML, Nakayama-Ratchford N, Davis CR, Kam NWS, Chu P, Liu Z, *et al*. A pilot toxicology study of single-walled carbon nanotubes in a small sample of mice. Nat Nanotechnol. 2008;3(4):216–21.
55. Garg M, Jain NK. Reduced hematopoietic toxicity, enhanced cellular uptake and altered pharmacokinetics of azidothymidine loaded galactosylated liposomes. J Drug Target. 2006;14(1):1–11.
56. Lu YJ, Wei KC, Ma CCM, Yang SY, Chen JP. Dual targeted delivery of doxorubicin to cancer cells using folate-conjugated magnetic multiwalled carbon nanotubes. Colloids Surf B Biointerfaces. 2012;89:1–9.
57. Singh R, Mehra NK, Jain V, Jain NK. Gemcitabine-loaded smart carbon nanotubes for effective targeting to cancer cells. J Drug Target. 2013;21(6):581–92.